Preliminary investigation into the extraction of light rare earth elements from different resources using the sulphation roasting process

K.C. Maluleke[1,2], X.C. Goso[1], S. Ndlovu[2,3], E. Matinde[1,2], and S. McCullough[4]

Affiliation:
[1]Pyrometallurgy Division, Mintek, Randburg, South Africa.
[2]School of Chemical and Metallurgical Engineering, University of the Witwatersrand, Johannesburg, South Africa.
[3]DST/NRF SARChi: Hydrometallurgy and Sustainable Development, University of the Witwatersrand, Johannesburg, South Africa.
[4]Techemet, Pasadena, Texas, USA.

Correspondence to:
K.C. Maluleke

Email:
malulekekgomotso@gmail.com

Synopsis

Rare earth elements (REEs) are commonly extracted from various resources using hydrometallurgical processes. However, these processes tend to be unselective, with high co-extraction of gangue components. Co-extraction of gangue elements is undesirable as it complicates downstream separation and purification processes. Preliminary tests were conducted on synthetic cerium oxide (chemical grade CeO_2) to investigate the technical feasibility of the sulphation roasting process for the extraction of REEs from different resources. Sulphation roasting was also applied to a REE-bearing ore under selected conditions. The highest REE extraction efficiency of 89% from synthetic CeO_2 was achieved under sulphation roasting conditions of 700°C over 24 hours in a gas atmosphere made up of 32% SO_2 and 16% O_2 (2:1, SO_2:O_2 ratio). The extraction efficiencies from the REE-bearing ore were 47% Ce, 46% La, and 67% Nd, 4% Fe, and 10% Mn after sulphation roasting at 750°C for 24 hours. These preliminary results indicate that it may be feasible to produce REEs from different resources using the established selective sulphation roasting process.

Keywords
rare earth elements, selective extraction, sulphation roasting.

Introduction

The rare earth elements (REEs) are a group of 17 metals consisting of 15 lanthanides, scandium, and yttrium, which have similar chemical properties. These metals are moderately abundant in the Earth's crust, with some more abundant than copper, lead, gold, and platinum (Humphries, 2011). The term 'rare' is a misnomer which is used to describe the REEs because they occur mostly in low concentrations in wide distributions. REEs do not occur naturally in their elemental state or as individual rare earth compounds. Instead, they occur as mixtures in various minerals (Gupta and Krishnamurthy, 2005).

All the lanthanides occur in nature except for promethium, which has no stable isotopes. The lanthanides with lower atomic numbers are more abundant in the Earth's crust than those with higher atomic numbers, while the lanthanides with even atomic numbers are two to seven times more abundant than the adjacent odd-numbered lanthanides (Castor and Hedrick, 2006). The lanthanides are divided into light, medium, and heavy REEs. The light REEs (LREEs), which include lanthanum, cerium, neodymium, and praseodymium, are characterized by lower atomic masses compared with the heavy REEs (HREEs) (Samson and Wood, 2005). The unique properties of the LREEs make them useful in a wide range of applications, including the manufacture of catalysts, magnets, and electronics. They are also utilized as components in the metallurgical and glass industries (Deloitte Sustainability, 2017).

LREEs generally occur in two minerals – bastnaesite and monazite (Habashi, 1997). China and the USA host the largest deposits of bastnaesite, while monazite is abundant in Australia, South Africa, China, Brazil, Malaysia, and India (Humphries, 2011). In 2017, China was reported to be the main supplier of REEs, with a global share of 95%; it was also the major consumer of these metals (Deloitte Sustainability, 2017). Owing to the anticipated increase in demand for REEs, countries like South Africa that contain significant reserves of LREE-bearing minerals can also contribute to the global supply.

Current extraction processes for REEs typically involve hydrometallurgical techniques, such as acid/alkaline baking as well as acid/alkaline roasting (Sadri, Fereshteh, and Ahmad, 2017). Although these processes achieve high REE recoveries, they tend to be unselective due to the co-extraction of gangue metals such as Fe, Mn, and Mg. This results in the need for multiple purification stages, which

Preliminary investigation into the extraction of light rare earth elements

are not only expensive but are tedious and result in complicated process flow sheets (Shuai *et al.*, 2017). Sulphation roasting is an industrial technology used for the selective production of base metals from complex mineral ores. Hence, it was attractive to test the feasibility of sulphation roasting as an alternative process to address the selectivity problem associated with the conventional REE production processes.

The current study was conducted to investigate the efficiency of the sulphation roasting process as an alternative process for the conversion of REE oxides (REEOs) to readily water-soluble REE sulphates. The study involved the calculation of predominance phase diagrams, using FactSage 7.3 thermochemical softwares (Bale *et al.*, 2009), for metal-gas systems to predict the stable phases at the different roasting temperatures. Preliminary sulphation roasting and leaching experiments were conducted on synthetic cerium oxide (CeO_2) and a REE-bearing ore.

Sulphation roasting

Sulphation roasting is a pyrometallurgical process utilized in the beneficiation of metal oxide ores to produce metal sulphates that are soluble in water or dilute mineral acids (Stanton, 2016). The process can be made selective by controlling variables such as the roasting temperature and gas partial pressures. Sulphation roasting is successfully utilized in the selective extraction of base metals such as copper and cobalt from iron-rich sulphide ores (Guntner and Hammerschmidt, 2012). Sulphation is usually achieved by heating the raw materials with sulphur trioxide (SO_3), made up of a stoichiometric mixture of sulphur dioxide (SO_2) and oxygen (O_2). The process can be carried out in a fluidized bed reactor, multiple hearth furnace, or a rotary kiln (Gutner and Hammerschmidt, 2012).

Reaction mechanisms

There is insufficient information in the public domain to show the applicability of this strategic process in the production of REEs. There is also uncertainty regarding the actual reactions that would take place during the sulphation roasting of REE-bearing materials.

The sulphation roasting of metal oxides in the presence of SO_2 and O_2 gases occurs in two main steps. The first step involves the oxidation of SO_2 gas by O_2 to form SO_3. This reaction is described by Equation [1] (Hanf, 1979; Guntner and Hammerschmidt, 2012).

$$SO_2 + 0.5O_2 \rightarrow SO_3 \qquad [1]$$

The second step involves the reaction between the metal oxides and SO_3 to form metal sulphates and/or basic sulphates. This reaction step is described by Equations [2] and [3] (Gutner and Hammerschmidt, 2012).

$$MeO + SO_3 \rightarrow MeSO_4 \qquad [2]$$

$$2MeSO_4 \rightarrow MeO.MeSO_4 \qquad [3]$$

The sulphation of REEs is predicted to follow the reaction described by Equation [4], determined from the predominance phase diagrams calculated using FactSage thermochemical software. The LREEs are very similar chemically and are thus expected to follow the same trend as cerium oxide.

$$2CeO_2 + 3SO_2 + O_2 \rightarrow Ce_2(SO_4)_3 \qquad [4]$$
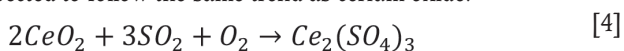
Thermochemistry

Temperature plays a vital role in the selectivity aspect of the sulphation roasting process and needs to be controlled within a narrow range to avoid decomposition of the formed sulphates (Sithole, Goso, and Lagendijk, 2017). The roasting temperature is selected based on the temperature requirement for the sulphation of the metals of interest as well as the temperature required for the decomposition of gangue metal sulphates. The roasting temperature in the study was in the range 600–800°C. Fe is the major gangue metal in the REE-bearing ore investigated in this study. Furthermore, Fe sulphates are known to decompose to haematite and SO_2 at temperatures above 600°C (Gutner and Hammerschmidt, 2012). The major gases present during the roasting process include SO_2 and O_2 in different ratios. At a fixed temperature, the proportions of these gases are determined by the partial pressures of SO_2 and O_2. The composition of the condensed phases is also dependent on the composition of the gas phase. Metal and gas systems for roasting processes are usually described using predominance phase diagrams. These diagrams are calculated to predict the products formed at the specific roasting temperature and gas partial pressures (pSO_2 and pO_2) (Safarzadeh and Howard, 2018).

Experimental

Material and samples

The cerium oxide (CeO_2), cerium (III) sulphate ($Ce_2(SO_4)_3$), and iron sulphate ($Fe_2(SO_4)_3$) used in the study were supplied by Merck. $Ce_2(SO_4)_3$ and ($Fe_2(SO_4)_3$) were used to evaluate their thermal stabilities in their arbitrary binary mixture. The N_2, O_2, and SO_2 used in this study were all of reaction grade and were supplied by Afrox.

The REE-bearing ore was supplied by the Hydrometallurgy Division of Mintek. This material was accompanied by the mineralogical and bulk chemical composition data summarized in Tables I and II respectively. In the current study, the bulk chemical compositions of the various samples were determined by inductively coupled plasma optical emission spectrometry (ICP-OES) (Spectro Ciros Vision) and inductively coupled plasma mass spectrometry (ICP-MS) (Perkin Elmer NexION 300Q). The sulphate content in the samples was determined by precipitation.

The phase chemical compositions of sulphated materials were determined by X-ray powder diffraction (XRD) using a Bruker D2 instrument. Only crystalline phases in sufficient amounts to diffract, usually not less than 5 mass %, are detectable through this method.

Equipment

A schematic representation of the horizontal tube furnace used in the test work is shown in Figure 1. The reactor is made up of a 30 mm diameter quartz tube, which is heated to a set temperature in a resistance-type furnace. A K-type thermocouple was placed next to the sample inside the furnace to monitor the sample temperature throughout the test. The furnace controller was connected to the sample thermocouple for automatic regulation of the furnace resistance to control the temperature (Sithole, Goso, and Lagendijk, 2017).

Thermochemical simulation

FactSage 7.2 thermochemical software (Bale *et al.*, 2009) was used to calculate the predominance phase diagrams in the

Preliminary investigation into the extraction of light rare earth elements

Table I

Phase chemical composition of the REE-bearing ore

Mineral	Formula	Grade
Goethite	FeO(OH)	Major
Haematite	Fe_2O_4	Major
Magnetite	Fe_3O_4	Major
Quartz	SiO_2	Major
Crandallite	$(Ca, Sr, Ba, Pb)Al_3(PO_4)(POß_3OH)(OH)_6$	Major
Mica	$K_2Mg_6Si_8O_{20}(OH)_4$	Major
Rutile	TiO_2	Trace
Ilmenite	$FeTiO_3$	Trace
Gypsum	$CaSO_4.2(H_2O)$	Trace
Barite	$BaSO_4$	Trace
Monazite*	$(Ce, La, Nd, Th)PO_4$	Trace
Cheralite*	$(Ce, Ca, Th)(P, Si)O_4$	Trace
Ce-pyrochlore	$(Ce, K)_2(NbTiFe)_2O_5F,OH$	Trace
REE-Apatite*	$(Ce, La, Ca)_5(PO_4)_3(OH, F, Cl)$	Trace
Florencite*	$CeAl_3(PO_4)_2(OH)_6$	Trace
Gorceixite	$BaAl_3(PO_4)_2(OH)_6$	Trace

Major: 20-50 mass %; trace: <5 mass %; determined by scanning electron microscopy (SEM) coupled with energy dispersive spectrometry (EDS). * REE phosphate

Table II

Bulk chemical composition of the REE-bearing ore

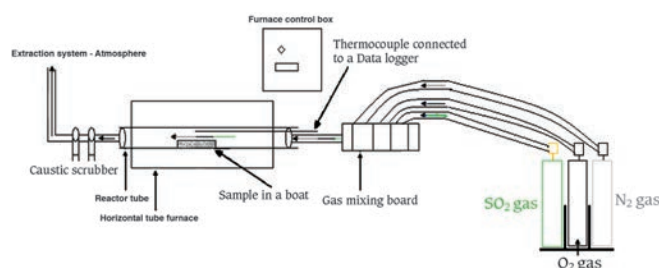| Element	ppm	Element	ppm	Element	%
Y	1 075.0	Li	49.7	Na	0.5
La	6 775.0	Be	56.3	Mg	0.8
Ce	10 944.0	V	617.0	Al	3.3
Pr	1 105.0	Cr	198.0	Si	3.5
Nd	3 812.0	Co	122.0	P	2.8
Sm	541.0	Ni	188.0	S	0.2
Eu	141.0	Cu	71.6	Ca	1.7
Gd	358.0	Zn	1 564.0	Ti	2.5
Tb	44.2.0	As	104	Mn	4.9
Dy	242.0	Cd	123	Fe	28.1
Ho	39.3	Pb	424	Sr	0.7
Er	146.3	Th	315	Ba	1.5
Yb	58.5	U	3.73		

Figure 1—Schematic representation of the sulphation roasting experimental set-up (Sithole, Goso, and Lagendijk, 2017)

temperature range of 630–800°C. This temperature range was chosen as it is in the range where gangue metal sulphates, such as Fe, start decomposing to metal oxides. The *predom* module of the software was used for these calculations. Factsage predominance phase diagram calculations are based on the Standard Gibbs free energy equations for the metals involved. Predomince phase diagrams were calculated to predict the stable products formed in the Ce-S-O and Ce-Fe-S-O systems at specific roasting temperatures. The two-metal systems are useful for determining the possibilities of selective sulphation.

These diagrams are also important in the study for deducing the probable process conditions that needed to be verified by empirical sulphation roasting tests.

Empirical sulphation roasting

For the sulphation roasting tests, discrete masses of 10 g of feed samples (synthetic CeO_2, mixed synthetic cerium (III) sulphate $(Ce_2(SO_4)_3)$ and iron sulphate $(Fe_2(SO_4)_3$, and REE-bearing ore) were weighed into sample boats. The sample boats were placed at the centre of the 30 mm quartz reactor in the horizontal tube furnace. SO_2, O_2, and N_2 gases were mixed and controlled using a gas mixing board that was connected to the furnace inlet. The total flow rate of gases was 300 standard cubic centimetres per minute (sccm) or $5.46 \times 10\text{-}6$ m³/s. The outlet of the reactor was connected to a double caustic scrubber (made up of 10% NaOH) to ensure that the surplus toxic SO_2 gas was not emitted directly to the atmosphere but reacted to form Na_2SO_4 in the solution. A summary of the test matrix is given in Table III.

The development of the roasting conditions was guided by the need for highly sulphated REEs under conditions where the base metal or gangue mineral sulphates were unstable to avoid simultaneous leaching of REE sulphates with gangue metal sulphates. The main parameters were roasting time, which was varied between 24 hours and 48 hours, and temperature, which was varied between 630°C and 800°C in a reaction gas composition of 16% O_2, 32% SO_2 (or 1:2 ratio of O_2 to SO_2), and 52% N_2. N_2 was used as a carrier gas – this option of a carrier gas offers an opportunity to make a preliminary assessment of the technical feasibility of sulphation when O_2 is supplied as a component in air.

The phase chemical compositions of the sulphated materials were determined by XRD. The bulk chemical compositions of the sulphated materials were determined by ICP-OES, ICP-MS, and precipitation. The sulphated materials were also subjected to leaching trials to establish the corresponding leaching efficiencies of the REEs after the respective tests.

Leaching of sulphated materials

The objective of these tests was to determine the sulphation efficiency of the roasted REE materials, *i.e.* to determine how much of the initial REE oxide had been converted into soluble sulphate and dissolved into solution. The leaching test work

Table III

Summary of sulphation roasting test conditions

Test	Test material		Reaction time (h)	Roasting temperature (°C)
Sulphation roasting of CeO_2				
1		CeO_2	24	630
2		CeO_2	48	630
3		CeO_2	24	700
4		CeO_2	48	700
5		CeO_2	24	750
6		CeO_2	48	750
7		CeO_2	24	800
8		CeO_2	48	800
Sulphate stability test: sulphation roasting of $Ce_2(SO_4)_3$–$Fe_2(SO_4)_3$				
9	$Ce_2(SO_4)_3$- $Fe_2(SO_4)_3$ (1:1 mass ratio)		24	750
Sulphation roasting of REE-bearing ore				
10	REE-bearing ore		24	630
11	REE-bearing ore		24	750

was conducted on the products from tests 1–8, 10, and 11 to study the effect of roasting time and temperature on the leaching efficiency of REEs as well as prominent gangue elements such as Fe and Mn. The same leaching methodology was used for the various samples.

The leaching tests involved leaching a known mass of sulphated material in water. The sulphated solid sample was transferred into a 250 mL glass reactor equipped with an overhead stirrer with pH and temperature control, and the leaching solution was added. The pH of the system was adjusted to 3.5–4.0 by adding 98% sulphuric acid. A hotplate was used to maintain the reactor contents at the required temperature. The pulp density of the slurry ranged between 2% and 10% (m/m). The tests were conducted at a temperature of 80°C for 4 hours, with hot water added every 30 minutes to make up losses due to evaporation.

At the end of each test the slurry was filtered in a vacuum filtration unit. The residue was dried at 50°C for 8 hours in an oven. The mass of the residue and volume of the filtrate were recorded, and the residue was subjected to chemical analysis. The efficiency of the extraction of the REEs was calculated using Equation [5].

$$\% \text{ REE extraction} = \frac{\text{Mass of REE in leachate}}{\text{Mass of REE in the feed}} \times 100 \quad [5]$$

Results and discussion

Predominance phase diagrams

Predominance phase diagrams were calculated to predict the phase relations that exist at specific temperatures and gas compositions. The axes on the predominance phase diagram depict the logarithms of the partial pressures of SO_2 and O_2 in the gas phase. The diagram is divided into areas or domains of stability of the various solid compounds of the metal, S, and O. The conditions for coexistence of two and three solid phases are indicated respectively by the lines and triple points on the diagram (Pelton, 2014).

Predominance phase diagrams for Ce-S-O systems at 600°C, 700°C and 800°C are shown in Figure 2, 3 and 4 respectively. These diagrams show that Ce can exist as a stable sulphate phase, $Ce_2(SO_4)_3$, at all these temperatures. The increase in temperature shows that the formation of the stable Ce-sulphate phase will require higher O_2 partial pressures, as shown by the shift of the $Ce_2(SO_4)_3$ region to the left. An increase in temperature also results in an increase in the number of stable Ce oxide and Ce sulphide phases at lower O_2 partial pressures as shown in Figure 4.

Sulphation roasting is used commercially to selectively convert metal oxides to metal sulphates. The regions of selectivity can be predicted from predominance phase diagrams calculated for multiple metal systems. Figure 5 shows the predominance phase diagram calculated for a Ce-Fe-S-O system at 750°C. Ce is the metal of interest, while Fe is the major gangue metal in the REE-bearing ore. Therefore, the stability regions for these metals are important in this study. Regions of selectivity are shown by the presence of stable Ce sulphate phases, while Fe is in its stable oxide forms. Figure 5 shows that selectivity in the roasting process can be achieved at relatively lower O_2 partial pressures and higher SO_2 partial pressures, where Ce is in the form of $Ce_2(SO_4)_3$ and Fe is in the form of FeS_2.

The diagrams are useful in narrowing down roasting temperatures through the prediction of stable phases of the metals of interest but not for determining operational conditions, such as roasting time, for the formation of these stable phases.

Mass change evaluation

The mass changes as a result of the sulphation roasting of the synthetic CeO_2 are shown in Figure 6, while the mass changes for the stability tests and the roasting of REE-bearing ore are tabulated in Table IV. A positive mass change indicates the sulphation of oxides, whereas a negative mass change is an indication of the decomposition of sulphates and the dehydration of the synthetic Fe and Ce sulphates.

The net mass change in the sulphation of synthetic CeO_2 (tests 1–8) is consistently and considerably positive, suggesting
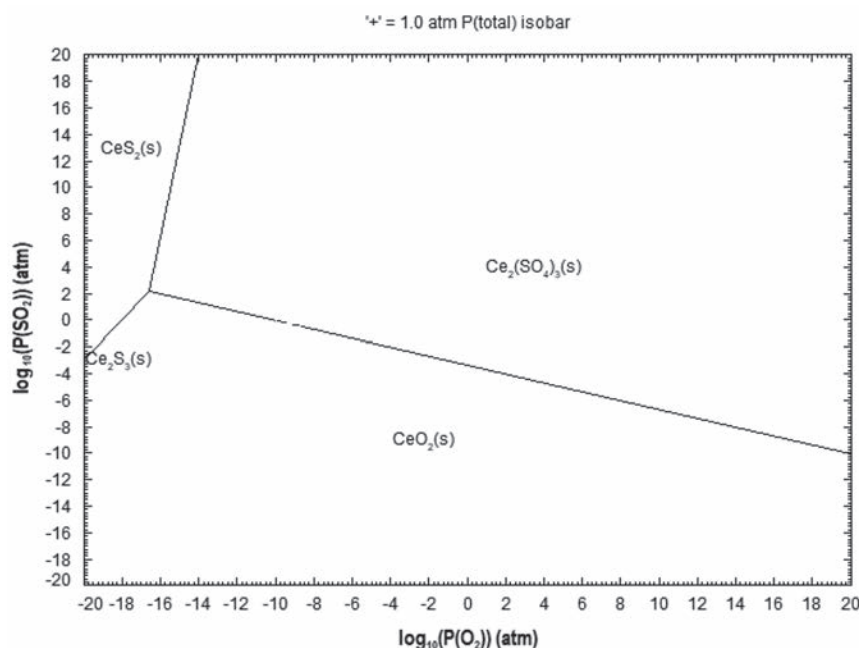

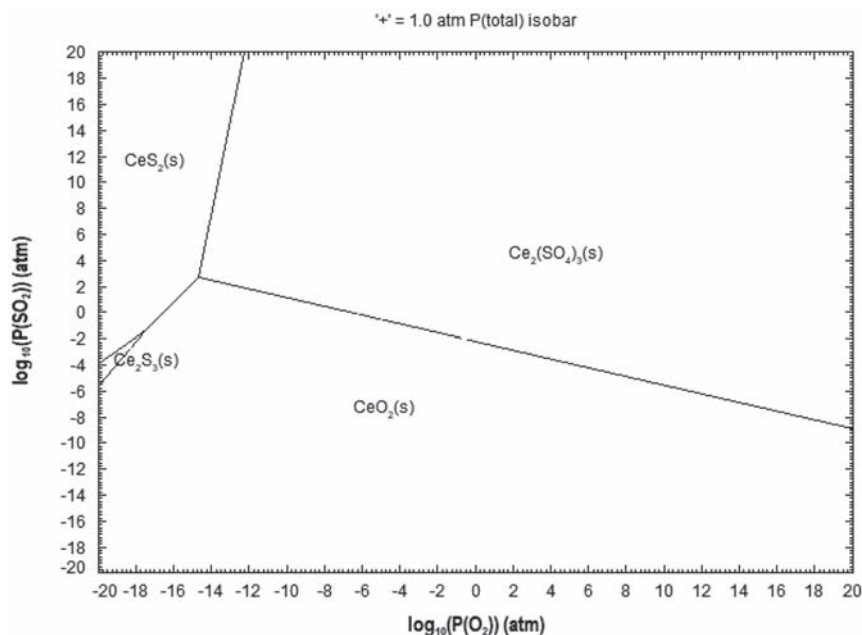Figure 2—Predominance diagram for the Ce–O–S system at 630°C

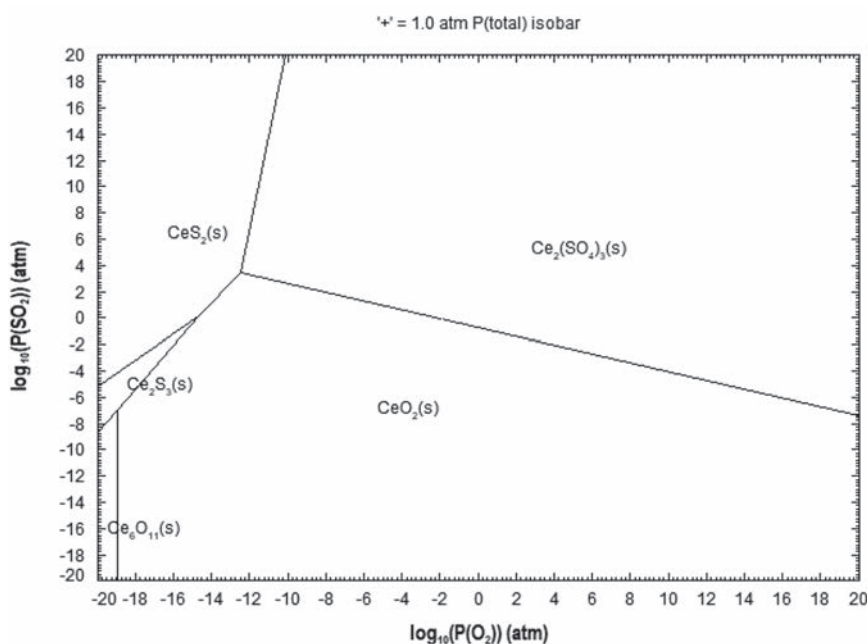Figure 3—Predominance diagram for the Ce–O–S system at 700°C

Figure 4—Predominance diagram for the Ce–O–S system at 800°C

significant sulphation of the oxides. The net mass changes are lower at lower roasting temperatures and roasting times. However, at 800°C the trend changes as the net mass change starts to decrease, suggesting that any Ce sulphates formed are becoming unstable and starting to decompose. The evaluation of the mass changes suggests that 750°C may be the temperature (for both 24- and 48-hour periods) for optimum sulphation, but the stability of the gangue sulphates needs to be evaluated.

The stability roasting test conducted on hydrated $Ce_2(SO_4)_3$ and $Fe_2(SO_4)_3$ at 750°C for 24 hours resulted in a negative net mass change. This was attributed to the dehydration of Ce and Fe sulphates and the decomposition of $Fe_2(SO_4)_3$ to Fe oxide. The net mass gain for the sulphation roasting of the REE-bearing ore sample was higher at 630°C than at 750°C.

The REE-bearing material contains significant amounts of Fe, which tends to be sulphated together with Ce during the roasting process. The higher net mass at lower temperatures (630°C) suggests the stability of Fe sulphates, and the decrease in the net mass at higher temperatures (750°C) suggests that the sulphates became unstable and decomposed to their oxides. The mass change of the ore at 630°C (25.2% mass change) follows a similar trend to that of the synthetic CeO_2 at the same temperature (23.2% mass change), which is an indication of applicability of the roasting conditions.

Mineralogical characterization

A summary of the phase chemical compositions of the sulphated synthetic CeO_2 is given in Table V. The phases are listed in order

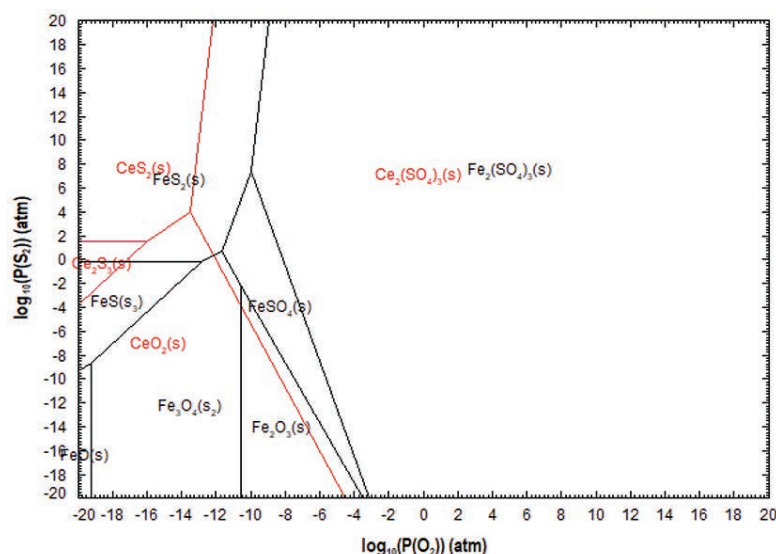# Preliminary investigation into the extraction of light rare earth elements

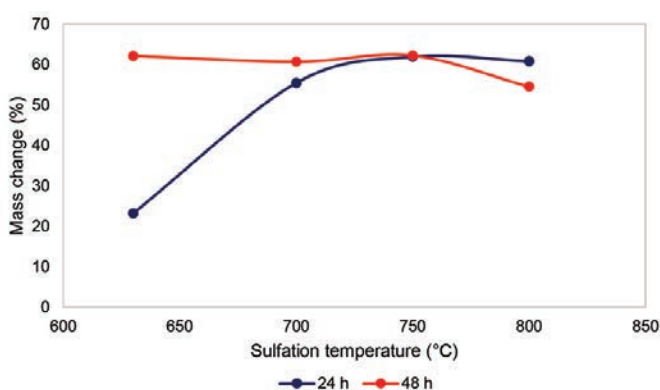**Figure 5—Predominance diagram for the Ce-Fe–O–S system at 750°C**

Figure 6—Graphical representation of mass changes for the sulphation of synthetic CeO₂ at different temperatures

Table IV

Summary of the mass changes for the stability tests and the sulphation of the REE-bearing ore

Material	Operational temperature (°C)	Roasting time (h)	Mass change (%)
$Ce_2(SO_4)_3$- $Fe_2(SO_4)_3$	750	24	-29.0
REE-bearing ore	630	24	25.2
	750	24	15.6

of decreasing abundance. The XRD results show the formation of cerium oxy-sulphate ($CeOSO_4$), and not a complete sulphate as predicted by FactSage. This phase was the dominant phase at all the sulphation roasting conditions studied for synthetic CeO_2. The presence of $CeOSO_4$ and CeO_2 phases is an indication of the decomposition of cerium (IV) sulphate ($Ce(SO_4)_2$), which occurs at temperatures between 400°C and 900°C. The products of sulphation roasting tests conducted at 630°C, 750°C, and 800°C also contained Ce as CeO_2, while $CeOSO_4$ was the only phase present at 700°C for both the 24-hour and 48-hour tests. The phases detected at 800°C are contrary to the findings by Poston *et al.* (2003), that only CeO_2 exists at this temperature (Poston *et al.* conducted the sulphation through the detrimental acid pasting and roasting procedure).

The XRD results for the sulphation of $Ce_2(SO_4)_3$ and $Fe_2(SO_4)_3$ at 750°C for 24 hours show the presence of $CeOSO_4$, Fe_2O_3, and $Fe_2(SO_4)_3$ (in order of decreasing abundance). This shows that $Ce_2(SO_4)_3$ decomposes to $CeOSO_4$, whereas $Fe_2(SO_4)_3$ is mainly decomposed to haematite after 24 hours. This suggests that selective sulphation can be achieved at 750°C as Ce is present mainly as a sulphate, while Fe is mainly present as haematite. The XRD results for the sulphation roasting of the REE-bearing ore sample are not reported because the individual rare earth oxides (REOs in the sample were below the detection limit of 5%.

Leaching of sulphated materials

Effect of sulphation temperature and roasting time on Ce leaching

The effect of sulphation roasting temperature on the leaching efficiency for synthetic CeO_2 is shown in Figure 7, and for the REE-bearing ore sample in Table VI. The leaching efficiency of Ce varied extensively with temperature. From the graph it can be noted that the leaching efficiency increased with increasing temperature from 630°C to 700°C for both sulphation roasting times. It was also noted that the leaching efficiency was higher for tests conducted for 24 hours than for those at 48 hours. The highest leaching efficiencies achieved at 700°C were 89% and 79% for sulphation conducted for 24 hours and 48 hours respectively. An increase in temperature to 750°C is associated with a decrease in the leaching efficiency in experiments conducted at both 24 hours and 48 hours. This is not consistent with the increases noted at 800°C.

Table V

Summary of the phase chemical compositions of the sulphated CeO₂

Temperature (°C)	REE products after 24 hours (order of decreasing abundance)	REE products after 48 hours (order of decreasing abundance)
630	$CeOSO_4$, CeO_2	$CeOSO_4$, CeO_2
700	$CeOSO_4$	$CeOSO_4$
750	$CeOSO_4$, CeO_2	$CeOSO_4$, CeO_2
800	$CeOSO_4$, CeO_2	$CeOSO_4$, CeO_2

Preliminary investigation into the extraction of light rare earth elements

As observed in Table VI, the sulphation roasting of the REE-bearing ore material at 630ºC did not result in any REE dissolution; however, an increase in the temperature to 750ºC resulted in 47% Ce, 46% La, and 67% Nd dissolution. Adversely, 4% Fe and 10% Mn dissolution also occurred. The presence of Fe and Mn in the solution is indicative of the co-sulphation of the gangue metals at a roasting temperature of 750ºC, which was predicted by the FactSage thermochemical calculations (Figure 4).

Conclusions

The technical feasibility of sulphation roasting as an alternative process for the conversion of rare earth element oxides (REEOs) to readily soluble REE sulphates was studied.

The predominance phase diagrams calculated for the Ce-S-O system between 630ºC and 800ºC showed that Ce can exist as a stable sulphate phase, $Ce_2(SO_4)_3$, at all these temperatures. However, an increase in temperature results in higher pO_2 requirements for the formation of this stable sulphate phase. The increase in temperature also shows the introduction of stable Ce-sulphide and oxide phases. The predominance phase diagrams for the Ce-Fe-S-O system at 750ºC showed a narrow region for selective conversion of Ce to $Ce_2(SO_4)_3$, while Fe was in a stable oxide phase.

XRD analysis of the sulphation roast products from processing synthetic CeO_2 revealed the formation of an oxy-sulphate phase, $CeOSO_4$, as the major phase at all the roasting temperatures. The presence of $CeOSO_4$ as well as CeO_2 is an indication of Ce sulphate decomposition.

The stability tests conducted on $Ce_2(SO_4)_3$ and $Fe_2(SO_4)_3$ at 750°C resulted in a negative net mass change, which indicates the possible dehydration and/or decomposition of the metal sulphates. XRD results of this test showed that that the abundant phases were $CeOSO_4$ and Fe_2O_3, with small quantities of $Fe_2(SO_4)_3$, indicating that selective sulphation is possible at this roasting temperature.

Mass changes calculated for the tests on synthetic CeO_2 were positive and relatively high for all the conditions in the study,
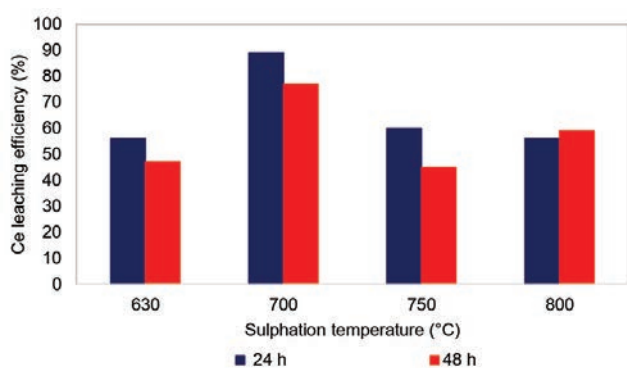

Figure 7—Graphical representation of the effect of sulphation temperature and roasting time on Ce leaching efficiency

Table VI

Summary of the leaching results for the REE-bearing ore sulphated for 24 hours

Operational temperature (°C)	Leaching efficiency (%)				
	Ce	La	Nd	Fe	Mn
630	0	0	0	0	0.7
750	47	46	67	4	10

while for the REE-bearing ore the mass change was higher at 630°C than at 750°C. The applicability of the roasting conditions obtained from the sulphation roasting of synthetic CeO_2 was shown by a similar trend in the mass change in synthetic CeO_2 at 630°C (23.2% mass change) and the REE-bearing ore (25.2% mass change) for experiments conducted at 630°C for 24 hours.

The highest leaching efficiency for synthetic CeO_2 roast products was 89% at 700°C after 24 hours. The leaching tests on the REE-bearing ore resulted in efficiencies of 47% for Ce, 46% for La, 67% for Nd, 4% for Fe, and 10% for Mn for tests conducted at 750ºC after 24 hours.

For further proof of the technical feasibility of the sulphation process for REE extraction, tests should be conducted on REE resources to determine the effect of the sulphation roasting time and temperature. The sulphation roasting mechanisms of REEs will also need to be investigated further to establish the actual reactions taking place during the process. Experiments should also be conducted in a fluidized bed set-up.

References

Bale, C.W., Bélisle, E., Chartrand, P., Decterov, S.A., Eriksson, G., Hack, K., and Robelin, C. 2009. FactSage thermochemical software and databases—recent developments. *Calphad*, vol. 33, no. 2. pp. 295–311.

Castor, S.B. and Hedrick, J.B. 2006. Rare earth elements. *Industrial Minerals and Rocks; Commodities, Markets.* Society for Mining, Metallurgy and Exploration, Littleton, CO. pp. 769–792

Deloitte Sustainability. 2017. British Geological Survey, Bureau de Recherches Géologiques et Minières, and Netherlands Organisation for Applied Scientific Research. 2017 study on the review of the list of critical raw materials. European Commission, Brussels.

Gutner, J. and Hammerschmidt, J. 2012. Sulphating roasting of copper-cobalt concentrate. *Journal of the Southern African Institute of Mining and Metallurgy*, vol. 112. pp. 455–460.

Gupta, C.K. and Krishnamurthy, N. 2005. Extractive Metallurgy of Rare Earths. 2nd edn. Taylor and Francis e-Library, New York.

Habashi, F. 1997. Handbook of Extractive Metallurgy. vol. 2. Wiley-VCH, Weinheim, Germany.

Hanf, N.W. and Schmidt, C.G. 1979. The roasting and leaching of Witwatersrand pyrite concentrates. *Journal of the South African Institute of Mining and Metallurgy*, vol. 79. pp. 365–371.

Humphries, M. 2011. Rare earth elements: The global supply chain. *Report no.* R41347. Congressional Research Service, Washington, DC.

Pelton, A.D. 2014. Thermodynamics and phase diagrams. *Physical Metallurgy*. Elsevier, Canada. Chapter 3.

Poston Jr, J.A., Siriwardane, R.V., Fisher, E.P., and Miltz, A.L. 2003. Thermal decomposition of the rare earth sulfates of cerium (III), cerium (IV), lanthanum (III) and samarium (III). *Applied Surface Science*, vol. 214, no. 1–4. pp. 83–102.

Sadri, F., Fereshteh, R., and Ahmad, A. 2017. Hydrometallurgical digestion and leaching of Iranian monazite concentrate containing rare earth elements Th, Ce, La and Nd. *International Journal of Mineral Processing*, vol. 159 (February). pp. 7–15.

Safarzadeh, M.S. and Howard, S.M. 2018. Solid state phase transformations during the oxidation of copper sulphides: Roaster diagrams for the Cu-S-O system. *Solid State Science*s, vol. 83. pp. 65–69

Samson, I.M. and Wood, S.A. 2005. The rare-earth elements: behaviour in hydrothermal fluids and concentration in hydrothermal mineral deposits, exclusive of alkaline settings. *Geological Association of Canada Short Course Notes*, vol. 17. pp. 269–297.

Shuai, G., Zhao, L., Wang, L., Long, Z., and Cui, D. 2017. Aqueous stability of rare earth and thorium elements during hydrochloric acid leaching of roasted bastnaesite. *Journal of Rare Earths*, vol. 35, no. 12. pp. 1255–1260.

Sithole, P., Goso, X.C., and Lagendijk, H. 2017. Laboratory-scale sulphation roasting testwork for copper and cobalt production. *Journal of the Southern African Institute of Mining and Metallurgy*, vol. 117. pp. 485–496.

Stanton, C.W. 2016. Sulfation roasting and leaching of samarium-cobalt magnet swarf for samarium recovery. Doctoral dissertation, Colorado School of Mines. Arthur Lakes Library. ◆